Materials Science Forum Vols. 329-330 (2000) pp 105-110
© (2000) Trans Tech Publications, Switzerland
doi:10.4028/www.scientific.net/MSF.329-330.105

Influence of Convection and Surface Effects on Macrosegregations in Eutectic and Peritectic Systems

G. Ehlen, A. Schweizer, A. Ludwig and P.R. Sahm

Gießerei-Institut, RWTH Aachen, Intzestraße 5, DE-52056 Aachen, Germany
Phone: +49-241-80-5882, Fax: +49-241-8888-276
E-Mail: georg.ehlen@gi.rwth-aachen.de

Keywords: Macrosegregation, Convection, Marangoni, Spot Welding, Line Welding, Oscillations, Algorithm, Phase Fractions

Abstract

The description of solute redistribution during welding processes is difficult due to a strong coupling between fluid flow, temperature field and macrosegregations. In this work a new stable algorithm for the calculation of melting and solidification in eutectic and peritectic binary alloys under extreme thermal conditions is presented. It uses piecewise linear eutectic and peritectic phase diagrams. It was applied to the simulation of thermal Marangoni convection and a transient line welding process. In both cases the development of the weld pool shape, the flow field and the carbon redistribution is predicted.

Introduction: Convection effects in welding processes

The numerical description of welding processes poses severe problems to the stability of the used algorithms. Especially when solute and heat redistribution by different convection effects is considered there is a complex system of strongly coupled differential equations that has to be solved simultaneously. Fig.1 shows the interactions that occur in thermal processes in general (a) and the extreme conditions and complex interactions that are typical for welding processes (b). The most important properties are extreme thermal conditions and high flow velocities. These conditions require a stable algorithm for solving the coupled equations.

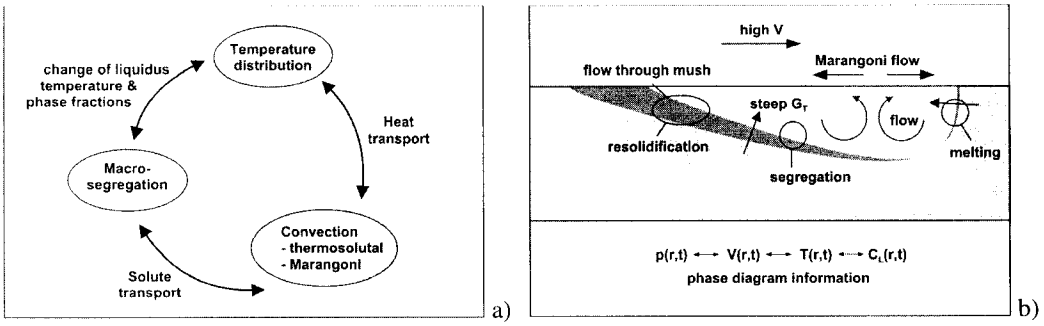

Fig. 1: a) Main interactions caused by convection effects during thermal processes in general. b) Physical phenomena governing transient welding processes.

The basic code

The convection effects have been modeled in a 2D FDM code based on the SIMPLER algorithm by Patankar [1] and the volume-averaged two-phase model of alloy solidification by Ni and Beckermann [2]. In addition to the calculation of fluid flow, heat and solute transport and the description of mushy zone flow by considering an anisotropic permeability of the dendritic region the new model has been extended to the following features: (i) a new stable algorithm for the calculation of eutectic and peritectic remelting and solidification of binary alloys (AlSi, FeC) using piecewise

All rights reserved. No part of contents of this paper may be reproduced or transmitted in any form or by any means without the written permission of the publisher: Trans Tech Publications Ltd, Switzerland, www.ttp.net. (ID: 193.170.16.107-26/01/10,15:23:09)

linear phase diagrams; (ii) surface tension driven Marangoni convection, implemented by a Cauchy-like boundary condition; (iv) temperature dependent physical data (iii) heat loss at the surface by vaporization.

A new stable algorithm for phase fraction / temperature update

The calculation of the phase fractions (ε_l, ε_s, ε_δ, ε_γ) for the new time step makes use of an iterative scheme presented by C. Prakash and V. Voller [3]. It couples energy and species conservation equations to find out the phase fractions, temperatures and concentrations for each control volume. Fig. 2 shows the situation for the case of primary γ-solidification (fraction solid $\varepsilon_s = \varepsilon_\gamma$, $\varepsilon_\delta = 0$). For each time step the discretized energy equation including conductive and convective terms leads to an expression for the new temperature that is a function of the new, unknown solid fraction ε_γ. A higher solid fraction represents a higher amount of latent heat released during the time step and thus a higher temperature $T(\varepsilon_\gamma)$. In the same way an expression for the liquid concentration can be set up as a function of ε_γ. The more depleted solid is built during the time step, the higher the resulting liquid concentration $C_l(\varepsilon_\gamma)$ must be. Thus each possible value of ε_γ is represented by a point in the T/C plane of the phase diagram, Fig. 2. The answer, which of these values for ε_γ will finally be realized, is given by the phase diagram and the condition, that for the correct ε_γ the temperature $T(\varepsilon_\gamma)$ must be the liquidus temperature at the liquid concentration $C_l(\varepsilon_\gamma)$: $T(\varepsilon_\gamma) = T_{liq}(C_l(\varepsilon_\gamma))$. Graphically this point is given by the intersection between the $T(\varepsilon_\gamma)$ / $C_l(\varepsilon_\gamma)$ - curve and the liquidus line of the phase diagram. Similar schemes have been established for eutectic and peritectic situations.

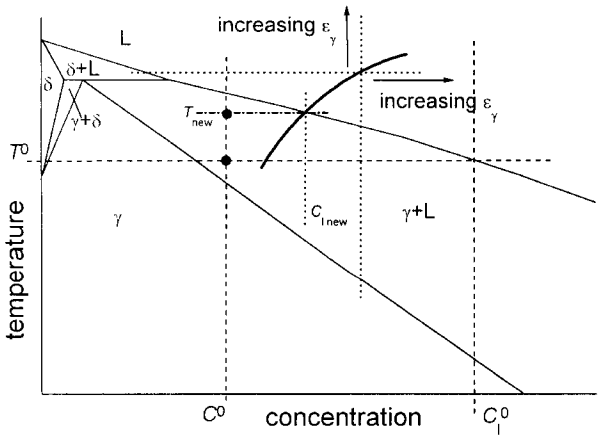

Fig. 2: Principle of the solid fraction / temperature updating scheme [3] for the solidification type primary γ-solidification. The thick solid line shows the possible T/C_l solutions for different solid fractions ε_γ. The correct solution is determined by the intersection of this line with the liquidus line of the phase diagram. Using the lever rule the solid fraction is given by

$$\varepsilon_\gamma = \frac{1 - \frac{C^0}{C_{l\,new}}}{1 - k}$$

The former algorithm, that was able to cope with cooling problems only, used temperature and liquid composition comparisons ($T < T_{liq}$, $T < T_{peri}$, C at the peritectic plateau etc.) to determine which solidification type was expected during the time step. In situations including both heating and cooling this decision gets much more complicated and conditions like $T > T_{peri}$ or $T < T_{peri}$ do not work any longer.

In a first step new conditions were introduced that could identify the solidification type. They used informations about the actual phase area *and* the existing phase fractions. When during the iterations of primary δ-solidification the algorithm stated that $T < T_{peri}$ *and* that there was still liquid phase left, it switched to the peritectic reaction. In the other direction when during primary γ-melting T became bigger than T_{peri} and there was still γ-phase left also the peritectic reaction was started. The end of peritectic melting or solidification was indicated by the disappearance of one of the three phases. This first version of the algorithm had some severe problems. Due to a couple of reasons the phase fraction calculation often meets exceptional and not well defined conditions that lead to erratic results. One of that reasons that is the semi-implicit formulation of the SIMPLER algorithm, another one is the fact, that the phase fraction algorithm is inserted in the outer SIM-

PLER iteration loop on the level of the relaxation procedure – where the temperature and velocity fields are not yet completely converged.

An algorithm had to be found that is independent from the degree of convergence. The new concept eliminates the temperatures and concentrations as the decisive values and uses the phase fractions themselves instead. Core of the new algorithm are the two *modules* for the calculation of primary δ/γ solidification/melting on the one hand, peritectic/eutectic solidification/melting on the other hand. They need all informations of the energy and liquid species equations as input and give the three phase fractions as output. They yield sure physically realistic solutions if the *resulting* temperature and concentration at the end of the time step is inside the correct phase area. But also if this condition is not fulfilled, the results give valuable information for further steps of the algorithm. If, for example, the system is inside the γ+L phase area and cools down, then the fraction of γ-phase will continuously go up. Without consulting the phase diagram we can determine the moment when the system is going to leave the γ+L phase area as the time step when the phase fraction module for primary solidification/melting indicates $\varepsilon_\gamma > 1$. Analogously the transitions from primary γ-solidification to peritectic reaction (peritectic module states: $1 > \varepsilon_\delta > 0$; $1 > \varepsilon_\gamma > 0$; $1 > \varepsilon_l > 0$) or from peritectic reaction to primary δ-solidification (peritectic module states: $\varepsilon_\gamma < 0$)can be identified. The principle of the new concept is to try out all possible solidification types and to decide from physical arguments which of the resulting phase fraction constellations is the correct one. For reasons of efficiency the conditions developed in the first version of the algorithm are used to give a rough estimation of the solidification type to be expected. Thus in most cases only one module has to be called to find out the physically correct solution. Only near phase lines two or three calls may become necessary.

The new algorithm was tested with several setups that included extreme temperature gradients, high flow velocities and strong segregation effects. It turned out to be stable for arbitrary paths inside the phase diagram. Fig. 3 shows an example for a complex melting and solidification path influenced by convective concentration drift.

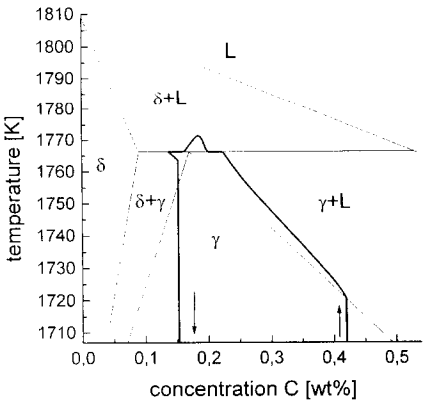

Fig. 3: Concentration drift inside one cell in a calculation of a spot welding process of steel with 0.42 wt% C. When the cell starts to melt up, solute is removed by convection and the mean C concentration is reduced. During the primary δ-melting the laser source is switched off and the cell starts to cool down. At the end of the peritectic resolidification the mean C concentration of the cell has been reduced so far that some δ-phase remains in the solid. The diagonal movement inside the δ+γ-area is due to the missing solid state transformation model.

Application I: Influence of Marangoni convection on spot welding

In a first application the code was used to simulate a spot welding process of steel with 0.42 wt% C. The aim was to investigate the influence of Marangoni convection on the weld pool shape and the development of macrosegregations. Marangoni convection is a surface flow that is driven by surface tension gradients. Surface tension can depend on temperature or solute concentration of surface active elements. The general Marangoni boundary condition at the surface is:

$$\tau_{xl} = \mu\left(\frac{\partial u}{\partial z}\right) = \left(\frac{\partial \gamma}{\partial T}\right)\left(\frac{\partial T}{\partial x}\right) + \sum_i \left(\frac{\partial \gamma}{\partial a_i}\right)\left(\frac{\partial a_i}{\partial x}\right) \qquad (1)$$

where τ_{st} is the shear stress in the surface layer, μ the dynamic viscosity, u the velocity parallel to the surface (x-axis), γ the surface tension, T the surface temperature and a_i the activity of the surface active element (here: S). The temperature dependence of the surface tension, $\partial\gamma/\partial T$, is the *Marangoni coefficient*. Three calculations were made with different constant values for $\partial\gamma/\partial T$ and one with a temperature dependent Marangoni coefficient using a semi-empirical equation by P. Sahoo et al. [4]. Fig. 4 shows the pool shapes and fully developed flow fields at the time when the laser source is switched off and the carbon macrosegregations after complete resolidification [5]. The pool shapes were compared to experimental investigations [6-8] and were found to be qualitatively correct.

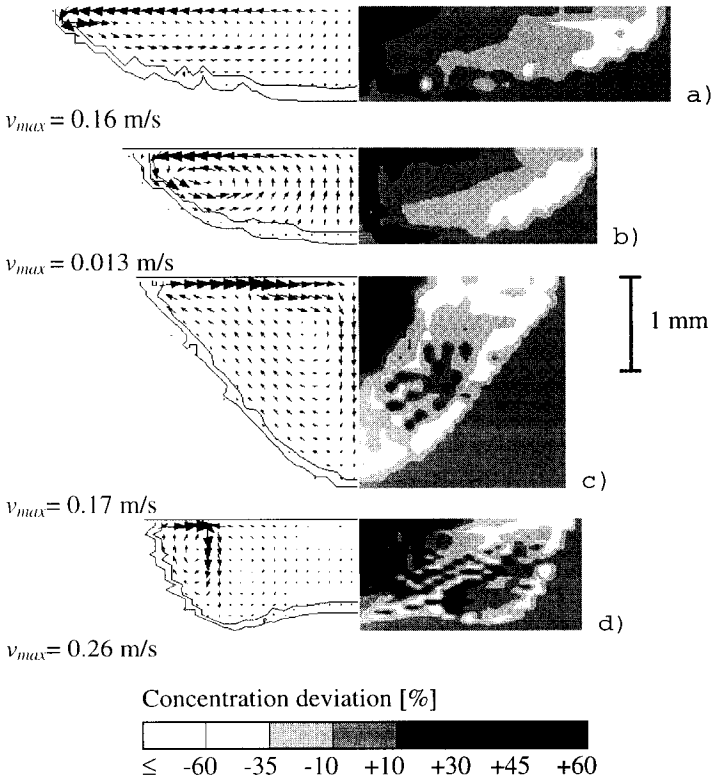

Fig. 4: Influence of different temperature dependencies of the surface tension. $\partial\gamma/\partial T$= *const.* taking the values a) -10^{-5} N/(m·K), b) 0, c) $+10^{-5}$ N/(m·K). d) $\partial\gamma/\partial T = f(T,a_S)$ using the equation developed by P. Sahoo et al. [4] with $\Delta H^0 = -1.88 \cdot 10^8$ J/mol and a sulfur activity a_S = 0.014. Left side: Shape of the weld pool and fully developed flow field after 3 s (notice the different maximal velocities); the border lines show the mushy zone with fraction solid between 0.3 and 0.98. Right side: Concentration deviation from the initial carbon concentration after total resolidification.
The sign of the Marangoni coefficient determines the direction of the surface flow. In case d) the sign changes in the outer part of the pool.

Application II: Macrosegregations in transient line welding

As a further application the question was treated how the concentration distribution could look like in the steady state of a line welding process. If there are any macrosegregation effects, there must be a depleted zone at the beginning of the weld and an enriched one at the end. For reasons of mass conservation the mean concentration of a cross section in the steady state between that must be equal to the initial composition. The aim was to determine i) how the spatial distribution in the cross section looks like and ii) how this steady state is reached.

Calculations were made on a 400×20 domain (100 mm × 5 mm) of a binary 0.1 wt% C steel. The laser source (P = 1.5 kW, efficiency = 80%) moved with v = 10 mm/s and was switched off after 9 s. The time resolution was Δt = 0.005 s. The Marangoni effect was not taken into account. To obtain realistic cooling conditions temperature dependent heat loss by vaporization at the surface was implemented using an equation by T. Zacharia et al. [9].

Fig. 5 shows three states of the transient calculation. The initial transient (after 1.3 s) shows an almost symmetric weld pool with two convection rolls. The carbon concentration inside the right roll

is almost equal to the initial concentration C^0. The solute that has been rejected by the resolidified area is collected inside the left roll. In the steady state (7.5 s) the weld pool has become non symmetric and shows an extended mushy zone at the left end. The carbon distribution in the pool qualitatively has not changed, but the concentration in the left convection roll has augmented. This has two consequences, Fig. 6 b): Even if at the bottom the resolidified weld is still depleted, curve b, the concentration a little above that has exponentially grown up and reached the initial concentration, curve m. At the surface a sequence of highly enriched areas has occured, that are separated by lightly depleted ones, curve t. In the (oscillating) steady state parts of the mushy zone are constricted periodically and the arising little pools concentrate the solute at the surface when they solidify separately. The final transient (10 s) shows a highly enriched area that is almost identical with the left convection roll. The right part is depleted and must have lost solute during solidification.

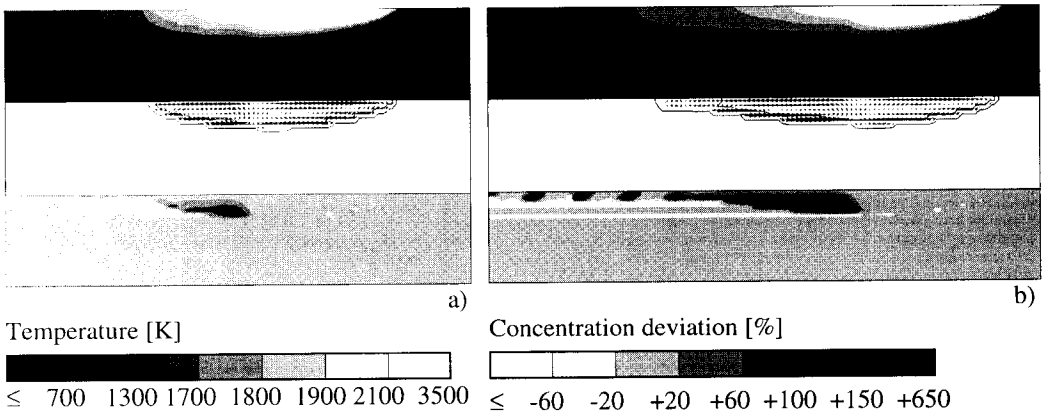

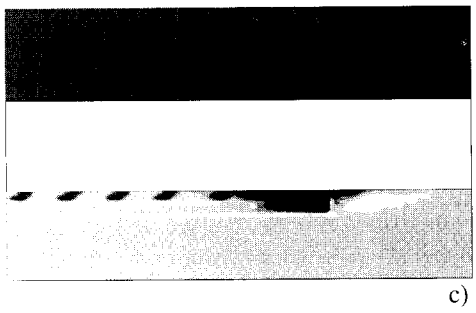

Fig. 5: a) Initial transient (after 1.3 s), b) steady state (7.5 s) and c) final transient (10 s) of a laser line welding process. From top to bottom: Temperature distribution; velocity field and fraction solid distribution, light grey: solid, dark grey: mushy zone ($0.02 < \varepsilon_s < 0.98$), white: liquid; concentration deviation from the initial carbon concentration.

The oscillations must be suspected to be numerical artefacts due to the discrete formulation of the algorithm that treats the melting or solidifying cell as a whole. Comparative calculations were made with different mesh resolutions. The oscillatory behaviour still occurred but with a different frequency. This could indicate, that in reality the mushy zone is very unstable, and this kind of segregations occurs, but maybe statistically distributed. The question remains how the distribution would look like when the oscillations were not physical. The periodical loss of highly enriched melt prevents the upper part of the pool from reaching the concentration level C^0 / k that would leave behind a resolidified area of concentration C^0. A non oscillating solidification would lead to a much more equilibrated steady state with smaller inhomogeneities. Fig. 6 c) shows an investigation of the long range carbon distribution. When the concentrations are integrated in y-direction and smoothed in x-direction the expected behaviour occurs: A depletion at the beginning that decreases exponentially until reaching the initial concentration (0.1 wt%) in the steady state, and a highly enriched zone at the end, followed by a little depleted one.

The description of the mushy zone is surely not yet accurate. In our case an estimation of the mushy zone extension at the right end of the pool gave a thickness of about 0.035 mm (∇T = 10^6 K/m, solidification interval 35 K). The cell size in this case was 0.25 mm. A good model of the mushy zone is essential for a quantitative description of segregation effects. An overestimation of the mushy zone size can result in concentraton deviations that are much too high. Due to the strong coupling between carbon concentration and liquidus temperature this can sensitively influence the shape and size of the pool.

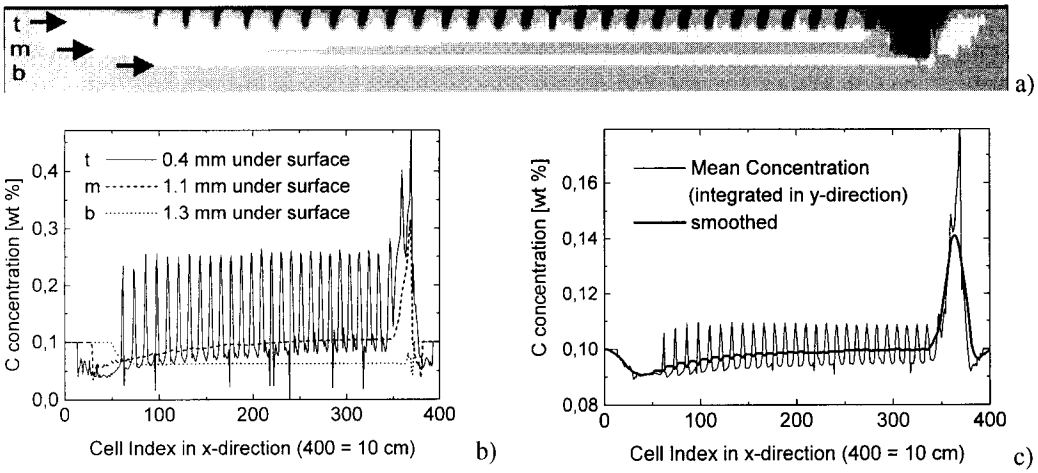

Fig. 6: a) Calculated concentration deviation from the initial carbon concentration (0.1 wt%) after total resolidification (vertical axis stretched). The arrows mark the positions of the horizontal line scans shown in b). c) Concentrations integrated in y-direction and smoothed in x-direction.

Conclusions and outlook

A new stable algorithm for the calculation of melting and solidification in eutectic and peritectic binary alloys under extreme thermal conditions was developed. It was applied to different welding processes. The simulation of Marangoni convection showed a strong dependence of the weld pool size and shape from the Marangoni coefficient. As a second application a transient line welding process was investigated. On a coarse scale the calculations show the expected carbon distribution. On a fine scale oscillations occured that are supposed to be numerical, but that might indicate an instability of the mushy zone. The program yields qualitatively senseful predictions of the carbon concentration during and after the welding processes. Further investigations have to treat the question of an accurate mushy zone model to make better quantitative predictions possible.

Acknowledgements

The work was supported by the *Deutsche Forschungsgemeinschaft* under grant №. Sa 335/30-1

References

1. S. V. Patankar, Numerical Heat Transfer and Fluid Flow, New York, Hemisphere (1980).
2. J. Ni, and C. Beckermann, Met. Trans. B, 22B (1991), p. 349-361.
3. C.Prakash, and H. Voller, Num. Heat Transf. B, 15 (1989), p. 171-189.
4. P. Sahoo, T. Debroy, and M.J. McNallan, Met. Trans. B, 19B (1988), p. 483-491.
5. G. Ehlen, A. Schweizer, A. Ludwig and P.R. Sahm, Modelling of Casting, Welding and Advanced Solidification Processes VIII, Warrendale, TMS (1998), p. 289-296.
6. Y.H. Xiao, and G. den Ouden, Mat. Sci. Technol. 13 (1997) p. 791-794.
7. C.R. Heiple and P. Burgardt, Weld. J. (Suppl.), 64 (1985), p. 159s-162s.
8. U. Dilthey and V. Pavlyk, Große Schweißtechnische Tagung, Hamburg (1998).
9. T. Zacharia, S.A. David, J.M. Vitek, Met. Trans. B, 22B (1991), p. 233-241.

Solidification and Gravity III
doi:10.4028/www.scientific.net/MSF.329-330

Influence of Convection and Surface Effects on Macrosegregations in Eutectic and Peritectic Systems
doi:10.4028/www.scientific.net/MSF.329-330.105

click for feedback
consult - comment - contact
consult comment contact
click for feedback